Proceedings of the Eleventh (2014) Pacific/Asia Offshore Mechanics Symposium **www.isope.org**
Shanghai, China, October 12-16, 2014

ISBN 978–1 880653 90-6: ISSN 1946-004X

Numerical Modelling of Poro-Elastoplastic Seabed under Combined Waves and Currents

*Y Zhang[1, 2, *], D-S Jeng[2], CC Liao[1], HY Zhao[2], JS Zhang[3]*
[1] Department of Civil Engineering, Shanghai Jiao Tong University, Shanghai, China
[2] Griffith School of Engineering, Griffith University Gold Coast Campus, Queensland, QLD, Australia
[3] State Key Laboratory of Hydrology-Water Resources and Hydraulic Engineering, Hohai University, Nanjing, Jiangsu, China
**Corresponding author*

ABSTRACT

This paper presents an integrated model for the wave(current)-induced seabed response. The Reynolds-Averaged Navier-Stokers (RANS) Equations and k-ε turbulence model are applied in the fluid field and the poro-elastoplastic model is used to simulate the seabed response. Validation of the present integrated model is presented first. Then the effect of currents on the seabed response is examined by considering both the oscillatory and residual mechanisms of the pore pressure inside the soil. A parametric study is conducted to examine the characteristics of the poro-elastoplastic model here. It shows that the development of the two-dimensional liquefaction zone can be illustrated by the present model. Besides, results show that opposite direction between waves and currents yields faster liquefaction process compared to the same direction.

KEY WORDS: waves and currents; seabed; poro-elastoplastic; oscillatory; residual.

INTRODUCTION

With growing activity in the marine environment, the phenomenon of wave-seabed interactions attracts great attentions among costal engineering since 1980s. A precise prediction of the excess pore pressure and liquefaction in a porous seabed is one of key factors in the design of foundation of marine installations.

In real marine environments, currents and waves exist simultaneously, and current is a main factor to the transportation and scouring above the seabed surface. For wave-current simulation, numerical models based on Navier Stokers equations have been widely developed since it could directly provide the solutions describing wave pattern and current state simultaneously. Park et al. (2001) proposed a numerical wave tank simulation with a finite-difference scheme and a marker-and-cell method to investigate wave motions and their interactions with steady uniform currents. Li *et al.* (2007) proposed a NS solver to simulate the interactions between breaking waves and a current over a cut-cell grid. And there exists many works have been done to explore the phenomenon of wave-current interactions(Kemp and Simons, 1982; 1983; Umeyama, 2009), but the effect of waves and currents on seabed response is still far away from understanding.

It has been well known that when waves propagated over the ocean surface, they exert dynamic pressures on the seabed sediment grains, which contribute to the changes of the pore pressures within the soil skeleton. Generally speaking, the mechanism of pore pressure changing can be divided into two categories (Zen and Yamazaki, 1990). One is oscillatory excess pore pressures with periodical response to waves, companied by amplitude damping and phase lag in pore pressure (Yamamoto *et al*., 1978). The other one is residual pore pressure which appears in the initial stage of the cyclic loading (Seed and Rahman, 1978). In this study, both of the two mechanisms will be considered.

It is obvious that simple elastic models for the seabed could not reveal the real soil characteristics, especially encountered with the build-up phenomenon of pore pressure which is caused by the soil plastic feature. On the other hand, the effect of cyclic shear stress cannot be ignored considering the cyclic characteristics of the ocean wave loadings. It was pointed out by Seed and Lee (1966) that the magnitude of cyclic stresses has influence on the build-up process of pore pressure. Seed and Rahman (1978) then studied the cyclic plasticity of soils under progressive wave and took into account the distribution of the cyclic shear stress in the soil profile as well as the important factor of pore pressure dissipation. Sumer and Cheng (1999), Jeng and Seymour (2007) developed an analytical solution for the build-up mechanism, respectively. Sekiguchi *et al*.(1995) derived an one dimensional closed-form poro-elastoplastic solution for the cumulative contraction of soils under cyclic loading of standing waves.

In addition to theoretical approaches, several series of experiments with respect to wave-induced pore pressure build up has been conducted. Sekiguchi et al.(1995), Sassa and Sekiguchi(1999) presented series of experimental results for the wave-induced residual pore pressure on the basis of centrifuge wave tank tests. Sumer *et al*. (2012) proposed an experimental study to find how pore pressures build up under both liquefaction and no-liquefaction regime.

In this study, a simple but workable two dimensional poro-elastoplastic model which includes the accumulation and dissipation of pore pressure would be conducted. With this model, the soil seabed response due to combined waves and currents would be investigated. . A parametric study carried out to investigate the effects of currents and soil characteristics. Furthermore, the liquefaction analysis would be conducted which supplies a better visualized demonstration of the

stability of the seabed.

THEORETICAL FORMULATIONS

In this study, the ocean waves are generated by an internal wave-maker model which is added beneath the ocean surface. Besides, the Reynolds-Averaged Navier-Stokes (RANS) Equations, VOF method and k-Ɛ turbulent model will be developed for the simulation of waves and currents fields. Then, the solutions of the dynamic fluid pressures and shear stresses are imposed on the boundary of the seabed as external forces. Based on the proposed model, the seabed responses would be further examined.

RANS Equations for Wave-current Mode

Assuming the fluid is incompressible, it could be described by RANS Equations, which include mass conservation equation and momentum conservation equation.

$$\frac{\partial \langle u_i \rangle}{\partial x_i} = 0 \tag{1}$$

$$\frac{\partial \rho_f \langle u_i \rangle}{\partial t} + \frac{\partial \rho_f \langle u_i \rangle \langle u_j \rangle}{\partial x_j} = -\frac{\partial \langle p \rangle}{\partial x_i} + \frac{\partial}{\partial x_j}\left[\mu\left(\frac{\partial \langle u_i \rangle}{\partial x_j} + \frac{\partial \langle u_j \rangle}{\partial x_i}\right)\right] + \frac{\partial}{\partial x_j}\left(-\rho_f \left\langle u_i' + u_j' \right\rangle\right) + \rho_f g_i \tag{2}$$

where $\langle u_i \rangle$ is ensemble mean velocity component, x_i is the Cartesian coordinate, ρ_f is fluid density, t is time, $\langle p_i \rangle$ is fluid pressure, μ is dynamic viscosity, and g is acceleration due to gravity. The Reynolds stress term, $-\rho_f \left\langle u_i' u_j' \right\rangle$ could be written in the following form.

$$-\rho_f \left\langle u_i' u_j' \right\rangle = \mu_t \left[\frac{\partial \langle u_i \rangle}{\partial x_j} + \frac{\partial \langle u_j \rangle}{\partial x_i}\right] - \frac{2}{3}\rho_f \delta_{ij} k \tag{3}$$

where μ_t is turbulent viscosity, k is turbulence kinetic energe(TKE) and δ_{ij} is Kronecker delta. Substituting Equation (3) to Equation (2) yields

$$\frac{\partial \rho_f \langle u_i \rangle}{\partial t} + \frac{\partial \rho_f \langle u_i \rangle \langle u_j \rangle}{\partial x_j} = -\frac{\partial}{\partial x_i}\left[\langle p \rangle + \frac{2}{3}\rho_f k\right] + \frac{\partial}{\partial x_j}\left[\mu_{eff}\left(\frac{\partial \langle u_i \rangle}{\partial x_j} + \frac{\partial \langle u_j \rangle}{\partial x_i}\right)\right] + \rho_f g_i \tag{4}$$

in which $\mu_{eff} = \mu + \mu_t$ is the total effective viscosity.

In the wave mode, the wave is generated through the internal wave-maker method which is presented by Lin and Liu(1999). A source function $S(x_i, t)$ was added to the mass conservation equation .

$$\frac{\partial \langle u_i \rangle}{\partial x_i} = S(x_i, t) \tag{5}$$

For the fifth-order Stokes wave applied in this study, the source term

$$S(x_i, t) = \sum_{j=1}^{5} \frac{2C}{A} a_j \cos j\left(\frac{\pi}{2} - \omega t - p_s\right) \tag{6}$$

where A is the area of the source region, C is the wave celerity, a_j is the wave amplitude, ω is the wave frequency, p_s is the phase shift constant.

Poro-elastoplastic Seabed Mode

The wave induced pore pressure could be divided into two components:

$$u_e = u_{e1} + u_{e2} \tag{7}$$

where u_e denotes the wave induced excess pore pressure at a fixed position, u_{e1} represents the oscillatory component, and u_{e2} represents the residual component.

Oscillatory Soil Response

Based on Biot's consolidation theory(Biot, 1941), the governing equation for the poro-elastic soil could be described as

$$G\nabla^2 u_s + \frac{G}{(1-2\mu_s)}\frac{\partial}{\partial x}\left(\frac{\partial u_s}{\partial x} + \frac{\partial w_s}{\partial z}\right) = -\frac{\partial u_{e1}}{\partial x} \tag{8}$$

$$G\nabla^2 w_s + \frac{G}{(1-2\mu_s)}\frac{\partial}{\partial z}\left(\frac{\partial u_s}{\partial x} + \frac{\partial w_s}{\partial z}\right) = -\frac{\partial u_{e1}}{\partial z} \tag{9}$$

where G is the shear modulus of seabed soil; (u_s, w_s) are the soil displacements in the x- and z- directions, respectively; μ_s is Poisson's ratio.

Considering the seabed as hydraulically isotropic with the same permeability K in all directions, the conservation of mass (Biot, 1956) leads to

$$\nabla^2 u_{e1} - \frac{\gamma_w n_s \beta_s}{K}\frac{\partial u_{e1}}{\partial t} = \frac{\gamma_w}{K}\frac{\partial \varepsilon}{\partial t} \tag{10}$$

where γ_w is the unit weight of pore water; n_s is the soil porosity; the compressibility of pore fluid β_s and the elastic volume strain of soil matrix ε could be defined as

$$\beta_s = \frac{1}{K_w} + \frac{1-S}{P_{w0}} \tag{11}$$

$$\varepsilon = \frac{\partial u_s}{\partial x} + \frac{\partial w_s}{\partial z} \tag{12}$$

in which K_w is the true modulus of elasticity of water(taken as $2\text{x}10^9$ N/m^2), S is the degree of saturation and P_{w0} is the absolute water pressure.

Residual Soil Response

Suppose that the total volumetric strain increment ($\Delta\varepsilon$) could be divided into two components (Sassa and Sekiguchi, 1999): elastic component ($\Delta\varepsilon_e$) and plastic component ($\Delta\varepsilon_p$),

$$\Delta\varepsilon = \Delta\varepsilon_e + \Delta\varepsilon_p \tag{13}$$

The elastic component ($\Delta\varepsilon_e$) could be represented by the vertical effective stress $\Delta\sigma'_v$ through the coefficient of volume compressibility of the soil m_v which could be expressed as

$$d\varepsilon_e = m_v d\sigma'_v \tag{14}$$

And the storage equation relevant to a deformable soil with an incompressible pore fluid can be written as

$$\frac{\partial \varepsilon}{\partial t} = -\frac{K}{\gamma_w}\left(\frac{\partial^2 u_e}{\partial x^2} + \frac{\partial^2 u_e}{\partial z^2}\right) \tag{15}$$

Combining these above two equations (14) and (15) together yields

$$-\frac{K}{\gamma_w}\left(\frac{\partial^2 u_e}{\partial x^2} + \frac{\partial^2 u_e}{\partial z^2}\right) = m_v\left(\frac{\partial \sigma_v}{\partial t} - \frac{\partial u_e}{\partial t}\right) + \frac{\partial \varepsilon_p}{\partial t} \tag{16}$$

When considering a whole wave cycle process, some of the time averages components comes to zero,

$$\Delta\overline{\sigma}_v = \overline{u}_{e2} = 0 \tag{17}$$

It then follows that,

$$\frac{\partial u_{e2}}{\partial t} = \frac{K}{m_v \gamma_w}\left(\frac{\partial^2 u_{e2}}{\partial x^2} + \frac{\partial^2 u_{e2}}{\partial z^2}\right) + \frac{1}{m_v}\frac{\partial \varepsilon_p}{\partial t} \tag{18}$$

As assumed by Sekiguchi (1995), the plastic volumetric strain ε_p under cyclic loading with a constant amplitude is a function of a continuously increasing damage parameter $\xi(t)$,

$$\varepsilon_p(\xi) = \varepsilon_p^{\infty} \cdot [1 - e^{-\beta\xi}], \qquad \xi(t) = \frac{\omega}{2\pi} t = \frac{t}{T} \tag{19}$$

where β is a parameter governing the rate of accumulation of plastic volumetric strain and ε_p^{∞} is the amount of plastic volumetric strain that is attained ultimately with ξ approaching infinity, it could be described in the following term (Sassa, 2001):

$$\varepsilon_p^{\infty} = R[e^{\alpha\chi} - 1] \tag{20}$$

when consider the two-dimensional problem, the cyclic stress ratio χ could be expressed as

$$\chi = \frac{\tau(x,z)}{\sigma'_{v0}(z)} \tag{21}$$

$$\sigma'_{v0}(z) = -(\gamma_s - \gamma_w)z \tag{22}$$

where $\tau(x, z)$ is the shear stress amplitude and σ'_{v0} is the initial vertical effective stress. Substituting equation (19) and (20) into equation (18) yields

$$\frac{\partial u_{e2}}{\partial \xi} = \frac{2\pi K}{\omega m_v \gamma_w}\left(\frac{\partial^2 u_{e2}}{\partial x^2} + \frac{\partial^2 u_{e2}}{\partial z^2}\right) + MR\beta e^{-\beta\xi}(e^{\alpha\chi} - 1) \tag{23}$$

$$M = \frac{1}{m_v} = -\frac{z}{d_s} M_d, \qquad -d_s \le z \le 0 \tag{24}$$

where M increases essentially linearly with increasing effective confining pressure. M_d represents the value of M at the bottom of seabed which is a material parameter.

Boundary conditions

To solve above governing equations, appropriate boundary conditions are required. As depicted in Fig. 1, the water depth is d_w, a steady current flow is first achieved across the whole fluid domain, then the desired waves are generated with wave height H and wave period T.

For the wave-current model, zero surface tension with $\partial k / \partial \vec{n} = \partial \varepsilon / \partial \vec{n} = 0$ is imposed on the air-water interface, and no-slip boundary is given on the solid surface. Besides, an uniform velocity is provided at the left-hand-side inflow boundary and a pressure outlet is given at the right-hand-side. For the seabed soil model, the pore pressure and the shear stress is equal to the pressure and stress obtained from the wave mode. The left-hand-side and right-hand-side boundary are considered to be zero-displacement since it is assumed far away from the concerned region. The bottom of the seabed is considered to be impermeable and rigid, and no displacement and vertical flow occur at this boundary.

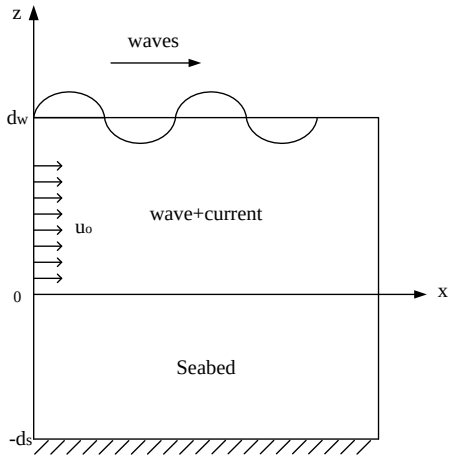

Fig.1 Problem definition for the system

Numerical method

In the wave-current interaction model, a two-step projection method is adopted for the mean flow solutions. The VOF (Volume of Fluid) method is used to track the free water surface. Time derivative is discretized by the forward time difference method. In the seabed mode, with the pressure and shear stress distributions obtained from the wave-current model, the oscillatory pore pressures and the cyclic stress ratio would be solved first. Then the results would be used to solve the equation (23) to get the residual pore pressures distribution.

MODEL VALIDATION

To validate the present wave-current interaction model, a comparison between the present study and the experiment result from Qi and Gao (2014) is presented. The experiment was conducted in a flow flume

which could generate waves and currents simultaneously with 52 m long, 1 m wide and 1.5 m high at the Institute of Mechanics, Chinese Academy of Sciences. A specially designed soil-box is located in the middle section of the flume, and the segment of 2.0m x 0.5m x 1.0m (length x depth x width) is employed in the experiment. Detailed information about the experiment could be found in Qi and Gao (2014).

Table 1. Parameters used in Qi and Gao(2014)'s experiment

Wave properties		
Wave height H(m)	Wave period T(s)	Current velocity u_0(m/s)
0.102	1.2	0.23
Soil properties		
Soil permeability K(m/s)	Relative density Dr	Buoyant unit weight of soil γ' (kN/m^3)
$1.88*10^{-4}$	0.352	9.03

With the same parameters of waves and currents Qi and Gao (2014) used in their experiment (Table 1), the pore pressure measured with PPT1 and PPT2 is compared with the numerical study in Fig. 2. It illustrates the pore pressure on the seabed surface and beneath the seabed surface in one period, respectively. In general, it could be seen from Fig. 2 that a good agreement existed between the simulated results and laboratory measurement which demonstrate the capacity of the present model in predicting the fluid motion when considering both of the waves and currents.

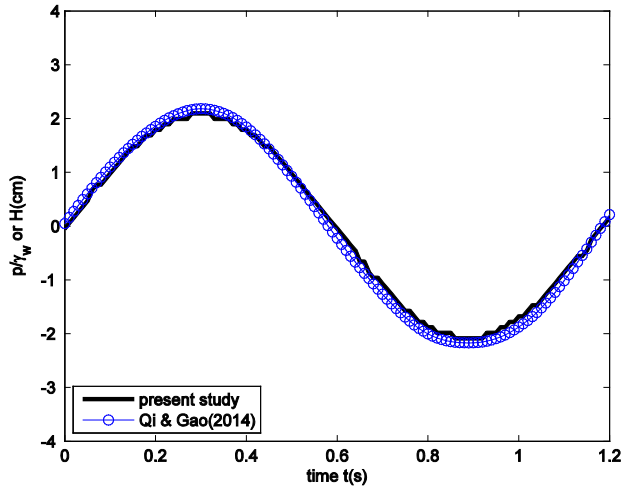

(a) z=0m.

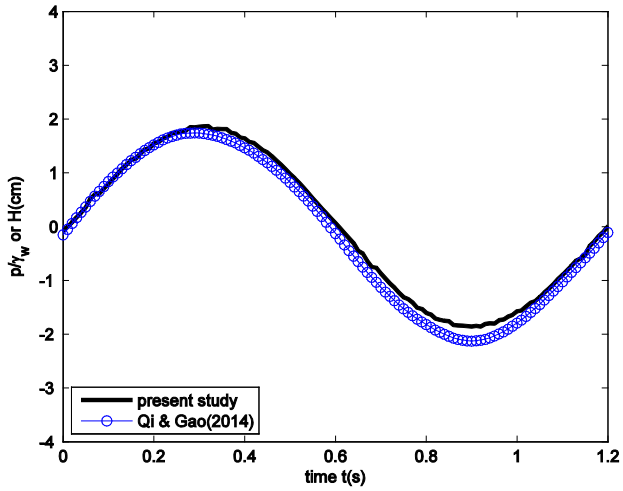

(b) z=-0.04 m

Fig.2 Comparison of simulated and measured pore pressure (PPT2) bellow the seabed surface.

The poro-elastoplastic seabed model is also validated through the comparison between the present results and the centrifuge data from Sassa and Sekiguchi(1999). Their experiment was conducted by using Leighton Buzzard sand under a centrifugal acceleration of 50g. Detailed parameters are listed in Table 2. It could be seen from Fig. 3 that the predicted results reveal the main features of the accumulation and dissipation of the pore pressure in the seabed.

Table 2. Parameters used in Sassa and Sekiguchi (1999)'s experiment

Wave properties		
Wave length L(m)	Wave period T(s)	Water depth d_w(m)
0.515	0.091	0.099
Soil properties		
Coefficient of permeability K(m/s)	Seabed Thickness h(m)	Degree of Saturation S
$1.5*10^{-5}$	0.1	1
Soil porosity n_s	Poisson's ratio μ_s	Shear Modulus G(N/m^2)
0.5	0.42	$5.4*10^5$
Material parameter α	Material parameter β	Material parameter R
55	0.04	$1.8*10^{-5}$

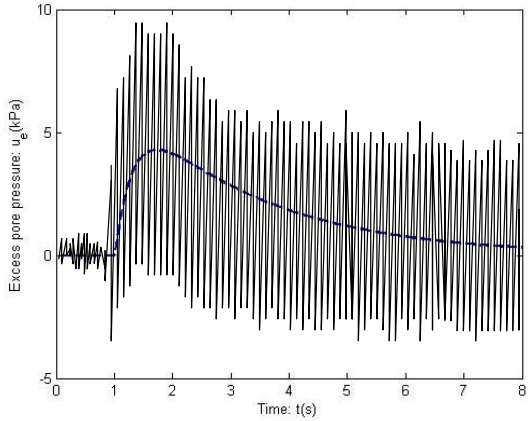

Fig.3 Comparison of present study and the results from Sassa and Sekiguchi (1999): -- the present solution; – Sassa and Sekiguchi (1999)

CONVERGENCE ANALYSIS

Before conducting a parametric study, it is necessary to do the convergence analysis of the model. A insufficient computation domain would result in the inaccuracy of the result, and too large computation domain requires huge computational time and memory of the computer. On the same way, mesh size also has an important influence to the computational result. In this study, the seabed model was tested for different domain sizes and mesh sizes. The input file for the test is listed in Table 3.

In this study, we consider three different LCD (length of the computation domain) for the simulation work, in which *L* is the wave length, and the oscillatory pore water pressure distribution at the center of the computation domain is illustrated in Fig. 4a. As shown in the picture, a computation domain with twice wave length is accurate enough for the simulation. In Fig. 4b and Fig. 4c, the build-up pore pressure distribution after one wave period and along 50 wave periods are illustrated, respectively. Four different MEZ (maximum element size [m^2]) which control the maximum allowed element size are consider in the study. It is obvious that when MEZ equals 1.3, both of the results from Fig. 4b and Fig. 4c are stable. In this study, the computation domain size exceeds twice wave length, and the maximum mesh size is chosen as 1.3.

Table 3. Input data for numerical examples

Wave properties		
Wave height H(m)	Wave period T(s)	Water depth d_w(m)
2	5	7.8
Soil properties		
Coefficient of permeability K(m/s)	Seabed Thickness h(m)	Degree of Saturation S
$1.0*10^{-6}$	30	1
Soil porosity n_s	Poisson's ratio μ_s	Shear Modulus G(N/m^2)
0.425	0.35	$5.0*10^6$
Material parameter α	Material parameter β	Material parameter R
50	0.04	$1.8*10^{-5}$

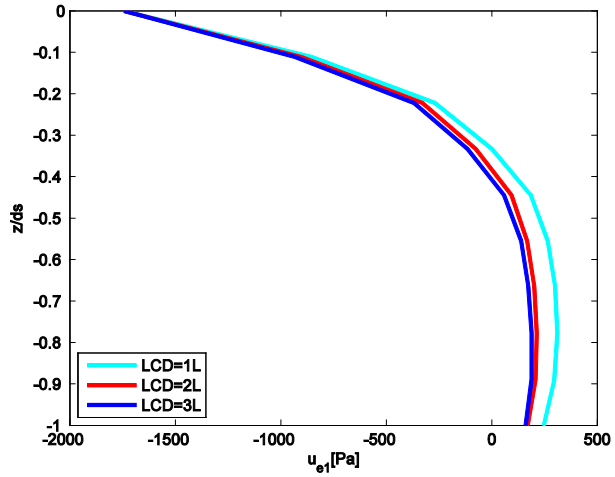

(a)

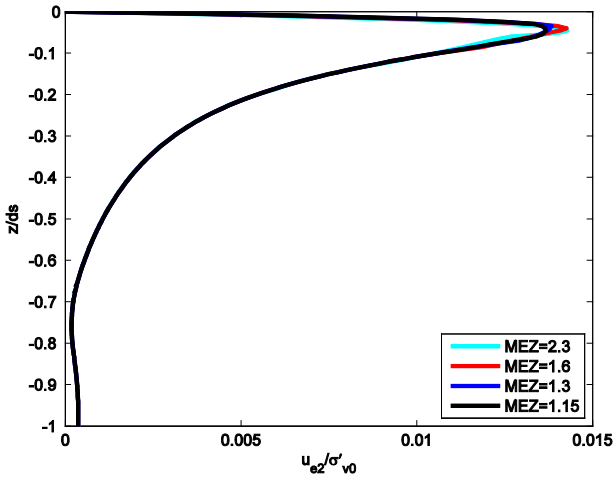

(b)

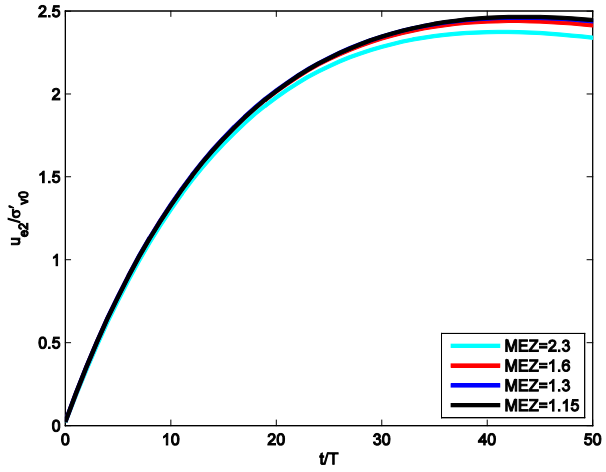

(c)

Fig. 4 (a) Domain test and (b) & (c) mesh tests

RESULTS AND DISCUSSIONS

Development of liquefaction zones

In this section, the liquefaction phenomenon will be examined by considering the poro-elastoplastic seabed model. The governing equation of the poro-elastoplastic model (equation (23)) leads the pore pressure owning two dimensional behavior as well as time-dependent character.

According to Sassa and Sekiguchi(1999), the liquefaction took place when the accumulated pore pressure reaches the value of the initial vertical effective stress,

$$u_{e2} = \sigma'_{v0}(z) \tag{25}$$

By applying this liquefaction criterion, the liquefaction development is plotted in Fig. 5. It clearly shows that the liquefaction zone behaves as a two dimensional pattern at the beginning of cyclic loading, and as the time goes, the two dimensional pattern gradually changed to one

dimensional. It can also be seen from Fig. 6 that the maximum liquefaction depth increases fast in the first 20 wave cycles, but gradually develop to a steady status. When the wave cycle number reaches about 50 (t/T=50), the liquefaction depth keeps at a constant number, which is about 4.3m.

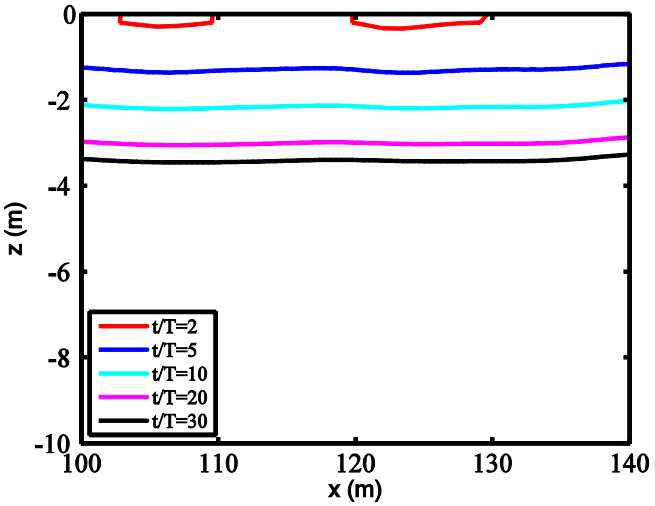

Fig. 5 The histories of development of liquefaction zone at different wave cycles

Effect of currents on wave profiles and seabed response

The current velocity (u_0) in present study are set variously from -1 m/s to 1 m/s with an interval of 0.5 m/s to explore the effect of current velocity on the wave height and wave length. The case of $u_0 \leq 0$ represents the case when waves travel against the current, and $u_0 \geq 0$ means waves travel following the current. The special case with $u_0=0$ stands for when waves travel alone and there is no current exists. As shown in Fig. 7, the waves travelling against the current result in a decrease in wave length and increase in wave height. On the contrary, the waves travelling follow the current lead to an increase in wave length and reduction in wave height.

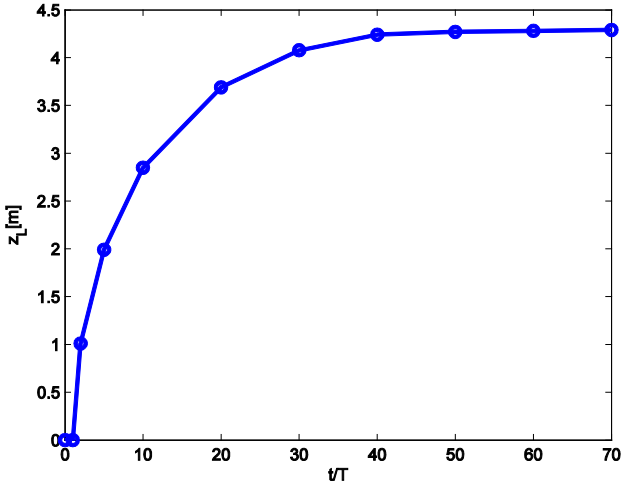

Fig. 6 The maximum liquefaction depth against the wave cycle number

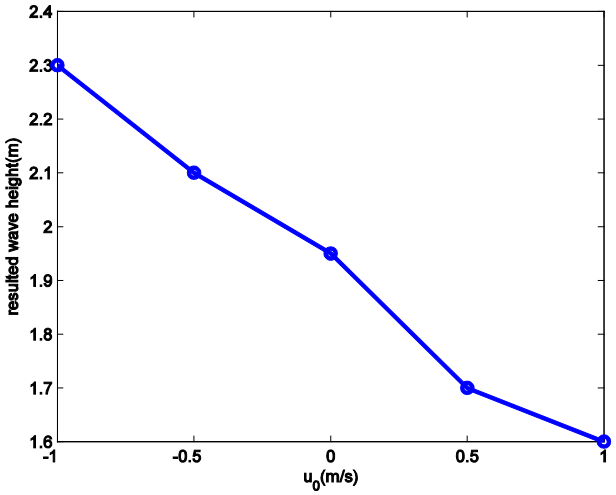

(a)

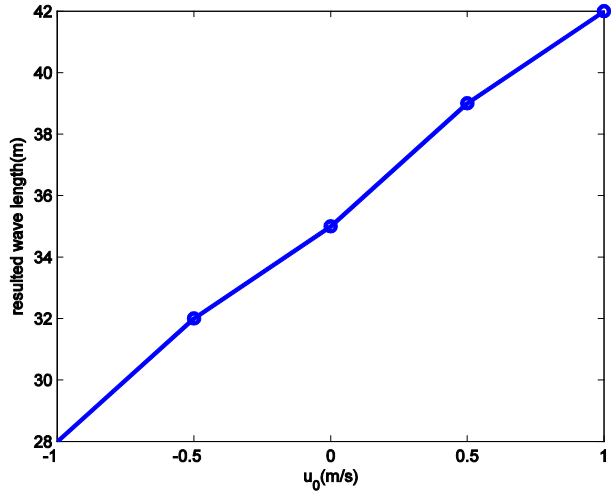

(b)

Fig. 7 Effect of current velocity on resulted (a) wave height and (b) wave length

The effect of the current on the soil response is examined here. As shown in Fig. 8, different values of u_{e2}/σ'_{vo} are depicted in z- direction. It is noted that liquefaction occurs when $u_{e2}/\sigma'_{vo}=1$. At a given time as $t/T=2$, liquefaction occurs in the case of u_0=-1m/s and u_0=0m/s, and no liquefaction appears when u_0=1m/s. The figure also implies that waves with opposite currents reach its liquefaction status faster than waves with following currents. It is obvious that the current velocity has a great influence on the distribution of accumulated pore pressures. In Fig. 9a, we choose three different value of current velocity to investigate the effect of the current on the pore water pressure accumulation and dissipation during 500 wave cycles. The results shows that the case of u_0=-1m/s reaches a higher peak of u_{e2}/σ'_{vo} and dissipates faster than the case when there is no current (u_0=0m/s). The case of u_0=1m/s has a smallest peak and dissipates slowly. In addition, It can be clearly seen from Fig. 9b that during 20 wave cycles periods, when wave travels against the current (u_0 =-1 m/s), it is faster for the soil at z=-2m to be liquefied, but to the case when wave travels along the current (u_0=1m/s), it shows a slower accumulation character.

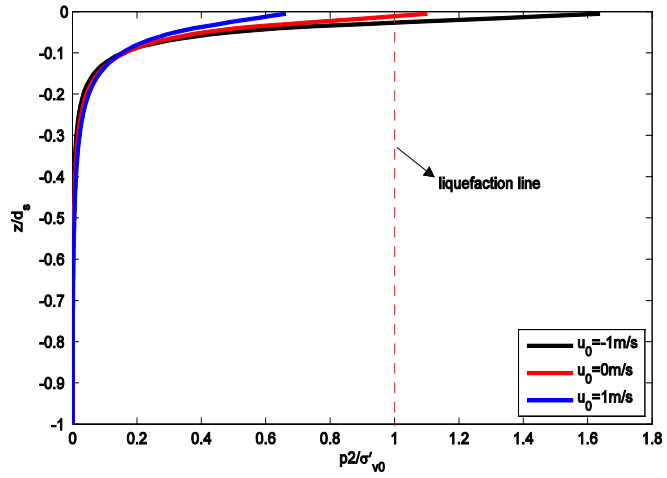

Fig. 8 Effect of current velocity on soil response in vertical direction after two wave periods(t/T=2).

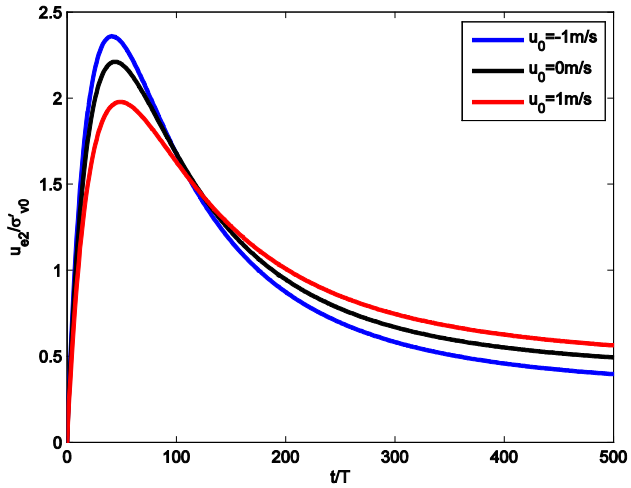

(a)

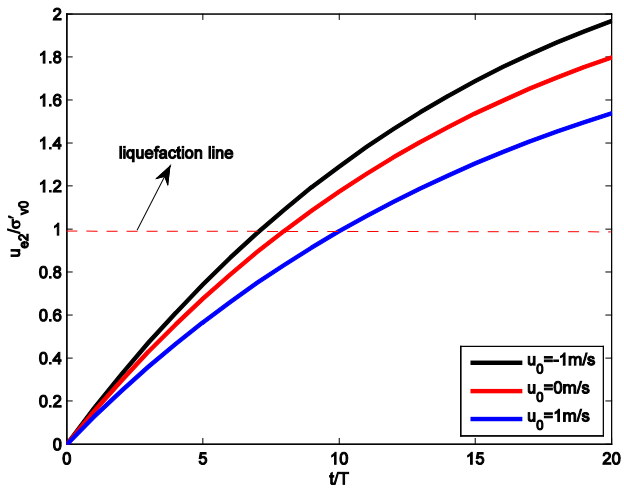

(b)

Fig. 9 Effect of current velocity on soil response during (a) 500 wave cycles and (b)20 wave cycles at z=-2m

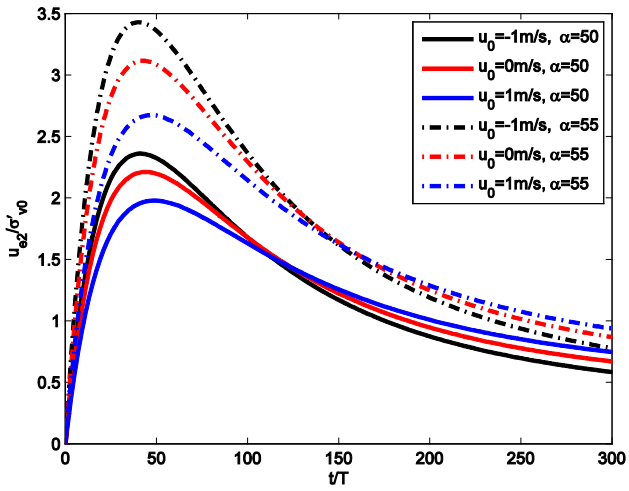

(a)

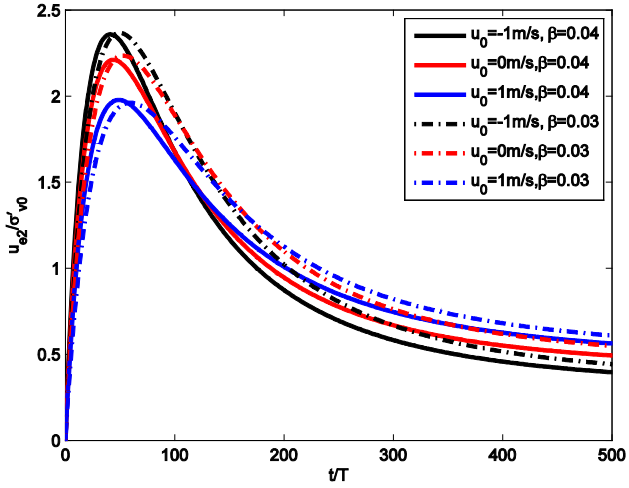

(b)

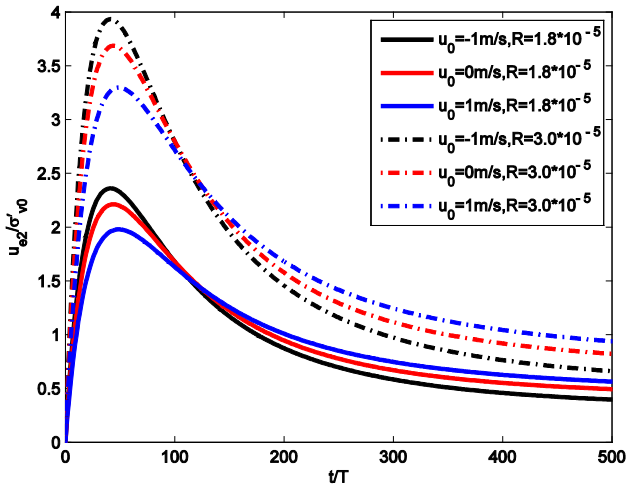

(c)

Fig. 10 Pore pressure accumulation and dissipation at z=-2m with various current velocity and material characteristic (a)α, (b)β and (c)R.

Effect of soil properties

In this study, a two dimensional poro-elastoplastic soil model is utilized to investigate the soil response under combined waves and currents. To further study the characteristics of this model, a parametric study is conducted to find out the most important material characteristic used in the model. As described in equation (23), the second term of the right-hand-side is called the source term, in which α, β and R are three important parameters which control the speed and the amplitude of the pore pressure accumulation. It can be found from Fig. 10 that α and R mainly control the amplitude of pore pressure accumulation, and β is the parameter governing the rate of the pore pressure accumulation and dissipation. The maximum values of u_{e2}/σ'_{vo} increases when α and R increases, and the speed to reach the maximum values of u_{e2}/σ'_{vo} decreases as β decreases.

CONCLUSIONS

In this study, the two dimensional poro-elastoplastic soil response under combined waves and currents is investigated after the validation and convergence analysis. Based on the results presented, it can be concluded that:

(1) The pore pressure accumulates and dissipates faster when waves travel against the currents, which means opposite direction between waves and currents makes the seabed liquefying process going faster than the same direction.

(2) Among the parameters used in the present poro-elastoplastic soil model, the residual parameters α and R control the amplitude of pore pressure accumulation, and β is mainly in charge of the rate of pore pressure accumulation and dissipation.

ACKNOWLEDGEMENTS

This study is supported by the State Scholarship Fund from China Scholarship Council.

REFERENCES

Biot, M. A. (1941). "General theory of three-dimensional consolidation." *Journal of Applied Physics*, Vol 26, No 2, pp 155–164.

Biot, MA. (1956). "Theory of propagation of elastic waves in a fluid-saturated porous solid, Part I: Low frequency range," *Journal of Acoustic Society, American*, Vol 28, pp 168-177.

Hirt, C. W., Nichols, B. D., (1981). "Volume of fluid(VOF) method for the dynamics of free boundaries." *J. Comput. Phys.* Vol. 39, pp 201-225.

Israeli, M., and Orszag, S. A. (1981). "Approximation of radiation boundary conditions." *Journal of Computational Physics.*, Vol 41, pp 115-131.

Jeng, D. S. and Seymour, B. R., (2007). "A simplified analytical approximation for pore-water pressure build-up in a porous seabed." *Journal of Waterway, Port, Coastal, and Ocean Engineering.* Vol. 133, pp 309-312.

Kemp, P. H., and Simons, R. R., (1982). "The interaction of waves and a turbulent current: waves propagating with the current". *Journal of Fuild Mechanics.* Vol. 116, pp 227-250.

Kemp, P. H., and Simons, R. R., (1983). "The interaction of waves and a turbulent current: waves propagating against the current". *Journal of Fuild Mechanics.* Vol. 130, pp 73-89.

Li, T., Troch, P., Rouck, J. D., 2007. "Interactions of breaking waves with a current over cut cells.", *J. Comput. Phys*. Vol. 223, pp 865-897.

Lin, P, and Liu, PL-F (1999). "Internal wave-maker for Navier-Stokes equations models," *Journal of Waterway, Port, Coastal, and Ocean Engineering, ASCE,* Vol 125, pp 207-415.

Park, J. C., Kim, M. H., Miyata, H., (2001). "Three dimensional numerical wave tank simulations on fully nonlinear wave-current-body interactions. J. Mar. Sci. Technol." Vol. 6, pp 70-82.

Qi W. G. and Gao F. P.,(2014). "Water flume modelling of dynamic responses of sandy seabed under the action of combined waves and current: Turbulent boundary layer and pore-water pressure". *The 8-th International Conference on Physical Modelling in Geotechnics(ICPMG2014).*

Sassa, S., and Sekiguchi, H., (1999). "Wave induced liquefaction of beds of sand in a centrifuge". *G´eotechnique*, Vol. 49, No. 5, pp. 621–638.

Sassa, S., Sekiguchi, H., and Miyamamot, J., (2001). "Analysis of progressive liquefaction as moving boundary problem". *G´eotechnique*, Vol. 51, No. 10, pp 847–857.

Seed, H. B., and K. L. Lee, (1966). "Liquefaction of saturated sands during cyclic loading." *Journal of the Soil Mechanics and Foundations Division, Proceedings of the American Society of Civil Engineers*, Vol 97, No SM9, pp 1249-1273.

Seed, H. B., and Rahman, M. S., (1978). "Wave-induced pore pressure in relation to ocean floor stability of cohesionless soils". *Marine Geotechnology*, Vol. 3, No. 2, pp 123–150.

Sekiguchi, H., Kita, K., and Okamoto, O., 1995. "Response of poro-elastoplastic beds to standing waves". , *Soils and Foundations.* Vol. 35, No. 3, pp 31–42.

Sumer, B. M. and Cheng N.S., (1999). "A random-walk model for pore pressure accumulation in marine soils." *The 9th International Offshore and Polar Engineering Conference (ISOPE99)*, Vol 1, pp 521-528.

Sumer, B. M., Kirca, V. S. O., and Fredsøe, J. (2012). "Experimental validation of a mathematical model for seabed liquefaction under waves." *International Journal of Offshore and Polar Engineering*, Vol. 22, pp 133–141.

Umeyama, M., (2009). "Changes in turbulent flow structure under combined wave-current motions". Journal of Waterway, Port, Coastal and Ocean Engineering, Vol. 135, pp 213-227.

Yamamoto, T, Koning, H, Sellmeijer, H, and Hijum, EV. (1978). "On the response of a poro-elastic bed to water waves," *Journal of Fluid Mechanics*, Vol 87, pp 193-206.

Zen, K., Yamazaki, H., 1990. Mechanism of wave-induced liquefaction and densification in seabed. *Soils and Foundations*. Vol. 30, pp90-104.

Zienkiewicz, OC, Chang, CT, and Bettess, P. (1980). "Drained, undrained, consolidating and dynamic behaviour assumptions in soils," *G´eotechnique*, Vol 30, pp 385-395.